Monthly Notices
of the
ROYAL ASTRONOMICAL SOCIETY

MNRAS **450,** 2094–2103 (2015) doi:10.1093/mnras/stv729

Chemical evolution of the Galactic Centre

V. Grieco,[1,2,3]★ F. Matteucci,[1,2,3] N. Ryde,[4] M. Schultheis[5] and S. Uttenthaler[6]

[1]*Dipartimento di Fisica, Sezione di Astronomia, Università di Trieste, Via G.B. Tiepolo 11, I-34143 Trieste, Italy*
[2]*INAF, Osservatorio Astronomico di Trieste, Via G.B. Tiepolo 11, I-34143 Trieste, Italy*
[3]*INFN, Sezione di Trieste, Via A. Valerio 2, I-34127 Trieste, Italy*
[4]*Department of Astronomy and Theoretical Physics, Lund Observatory, Lund University, Box 43, 221 00, Lund, Sweden*
[5]*Observatoire de la Côte d'Azur, CNRS UMR 7293, BP4229, Laboratoire Lagrange, F-06304 Nice Cedex 4, France*
[6]*Department of Astrophysics, University of Vienna, Türkenschanzstraße17, A-1180 Vienna, Austria*

Accepted 2015 March 30. Received 2015 March 12; in original form 2014 February 10

ABSTRACT

In recent years, the Galactic Centre (GC) region (200 pc in radius) has been studied in detail with spectroscopic stellar data as well as an estimate of the ongoing star formation rate. The aims of this paper are to study the chemical evolution of the GC region by means of a detailed chemical evolution model and to compare the results with high-resolution spectroscopic data in order to impose constraints on the GC formation history. The chemical evolution model assumes that the GC region formed by fast infall of gas and then follows the evolution of α-elements and Fe. We test different initial mass functions (IMFs), efficiencies of star formation and gas infall time-scales. To reproduce the currently observed star formation rate, we assume a late episode of star formation triggered by gas infall/accretion. We find that, in order to reproduce the [α/Fe] ratios as well as the metallicity distribution function observed in GC stars, the GC region should have experienced a main early strong burst of star formation, with a star formation efficiency as high as $\sim$25 Gyr^{-1}, occurring on a time-scale in the range $\sim$0.1–0.7 Gyr, in agreement with previous models of the entire bulge. Although the small amount of data prevents us from drawing firm conclusions, we suggest that the best IMF should contain more massive stars than expected in the solar vicinity, and the last episode of star formation, which lasted several hundred million years, should have been triggered by a modest episode of gas infall/accretion, with a star formation efficiency similar to that of the previous main star formation episode. This last episode of star formation produces negligible effects on the abundance patterns and can be due to accretion of gas induced by the bar. Our results exclude an important infall event as a trigger for the last starburst.

Key words: Galaxy: abundances – Galaxy: evolution.

1 INTRODUCTION

In the last years there has been an increasing interest in studying the Galactic bulge resulting from the accumulation of more spectroscopic data. In particular, from these data a rather complex picture for the bulge formation arose: the existence of at least two main stellar populations in the bulge was suggested by several studies (Babusiaux et al. 2010; Bensby et al. 2011, 2013; Gonzalez et al. 2011; Hill et al. 2011; Robin et al. 2012; Uttenthaler et al. 2012). The two populations arising from the spectroscopic data are characterized by a metal-poor (MP) one, with characteristics typical of stars belonging to a spheroid, and another one more metal-rich and with characteristics of bar kinematics. Also the [α/Fe] ratios of these two populations seem different in the sense that the metal-rich population shows lower [α/Fe] ratios (Hill et al. 2011). Grieco et al. (2012, hereafter GMPC12) tried to model these two populations and concluded that the MP population formed on a very short time-scale by means of an intense burst of star formation, whose efficiency was a factor of 20 higher than in the Galactic thin disc. The more metal-rich population instead should have formed on a longer time-scale and with lower star formation efficiency and it was created by the bar evolution. While in the GMPC12 model the bulge was treated as a unique single zone with radius of 2 kpc, here we present a model for the central region of the bulge, the Galactic Centre (GC). In particular, we will focus on a region of 200 pc radius. The GC region has an extremely rich environment: intense star formation with formation of a bulk of massive stars and three of the most massive young star clusters in the Galaxy. In the last years, many assumptions have been made about the nature of the

★ E-mail: grieco@oats.inaf.it

inner population and on the possible causes of the star formation activity in the last few hundred million years. Genzel et al. (2006) pointed out that most of the stars in the GC seem to have formed 9 ± 2 Gyr ago, probably at the same time as the Galactic bulge. Then the star formation rate (SFR) dropped to a minimum a few Gyr ago rising again in the past few million years. The star formation history was derived in the GC from the H–R diagram of the red giants (Pfuhl et al. 2011), while the present time SFR was derived from the infrared luminosity of the young massive stars forming in the large reservoir of molecular gas present in the GC (Yusef-Zadeh et al. 2009) or by counting these young massive stars (Immer et al. 2012). One important issue relevant to the nature of the stellar populations in the GC is the possible presence of a second bar. However, the presence of a double bar in our Galaxy, similar to what can be observed in external galaxies (Laine et al. 2002; Erwin 2004) is still under debate. Alard (2001), Nishiyama et al. (2005) and Gonzalez et al. (2011) claim that there is an inner structure distinct from the large-scale Galactic bar, with a different orientation angle which could be associated with a secondary, inner bar. On the other hand, Gerhard & Martinez-Valpuesta (2012) can explain this inner structure by dynamical instabilities from the disc without requiring a nuclear bar. Very recently, Ryde & Schultheis (2015) have measured, from high-resolution infrared spectroscopy, abundances of Mg, Si, Ca and Fe in nine M-type giants in the GC region. They found a metal-rich population at [Fe/H] $= +0.11 \pm 0.15$ dex with rather low [α/Fe] ratios with the possible exception of Ca. Their metallicity distribution function (MDF) is peaked at an [Fe/H] slightly higher than solar and agrees with previous data of Cunha et al. (2007). Cunha et al. (2007) had also measured high-resolution infrared spectra for a sample of cool stars within 30 pc from the GC; their results showed that [O/Fe] and [Ca/Fe] are enhanced by 0.2 and 0.3 dex, respectively. They also found that the total range in [Fe/H] in the GC is narrower than that found for the older bulge population.

The aim of this paper is to compare our results with the data of Ryde & Schultheis (2015) in order to impose constraints on the formation and evolution of the GC. The analysis of the abundance ratios, such as [α/Fe] ratios, versus [Fe/H] can allow us to understand the time-scale of the process of formation of the GC region. In fact, [α/Fe] ratios can be used as cosmic clocks because of the time-delay model. The time-delay model is the common interpretation of abundance patterns in terms of different chemical elements produced from different stars and on different time-scales. In this context, starting from the fact that α-elements are produced on short time-scales by core-collapse SNe, whereas Fe is produced partly in core-collapse SNe but mainly in Type Ia SNe exploding on longer time-scales, we can interpret the observed abundances. High [α/Fe] ratios at low [Fe/H] indicate that the star formation period was short enough to prevent the Type Ia SNe from polluting heavily the gas with Fe. On the other hand, we always expect that the [α/Fe] ratios are lower at high [Fe/H] because of Type Ia SN contribution. However, due to the combination of the SFR and the time delay in element production, objects where the SFR has been very intense show high [α/Fe] ratios up to even solar [Fe/H] values. This is because α-elements and part of Fe are produced fast by core-collapse SNe, which are able to enrich substantially the interstellar medium (ISM) in Fe before the bulk of this element is restored by SNe Ia (see Matteucci 2012). Therefore, the comparison between observed and predicted abundances can tell us about the history of the chemical evolution of the GC and in particular on the origin of its stellar populations. To perform such a comparison, we adopt a model very similar to that presented in GMPC12, in particular the model describing the classical bulge population which formed on a short time-scale as a result of an intense burst of star formation (the population called metal poor), applied to a central region of only 200 pc of radius. In order to reproduce the star formation observed at the present time, we also overimpose on the history of star formation, deriving from our model, a recent burst producing the same quantity of stars that have been observed.

The paper is organized as follows: in Section 2, we describe the chemical evolution model, in Section 3, we describe the stellar spectroscopic data as well as the SFR estimates. In Section 4, we present our results and the comparison with data. In Section 5, we draw some conclusions.

2 THE CHEMICAL EVOLUTION MODEL

The chemical evolution model we adopt here is the model of GMPC12 for the MP stellar population in the Galactic bulge. In other words, it is the model assuming a strong initial burst of star formation triggered by the heavy gas infall coming from the initial collapse that gave rise to the halo and the bulge. This model has been adapted here to the small central region around the GC. The assumed gas accretion law is

$$\dot{\sigma}_{\mathrm{gas},i}(t) = A(r) X_{i,\mathrm{inf}} \mathrm{e}^{-t/T_{i,\mathrm{inf}}}, \quad (1)$$

where i represents a generic chemical element, $T_{i,\mathrm{inf}}$ is an appropriate infall time-scale fixed by reproducing the observed stellar MDF and $A(r)$ is a parameter constrained by the requirement of reproducing the current total surface mass density in the central region of the Galactic bulge; in particular, we assume a present time surface mass density at $r = 200$ pc, $\sigma_{\mathrm{GC}}(200, t_{\mathrm{G}}) \sim 3.9 \times 10^5\,\mathrm{M}_{\odot}\,\mathrm{pc}^{-2}$, with $t_{\mathrm{G}} \sim 14$ Gyr being the lifetime of the Galaxy, and r the Galactocentric distance. We have obtained this value by assuming a mass distribution in the bulge which follows a Sersic (1968) profile. The quantity $X_{i,\mathrm{inf}}$ is the abundance of the element i in the infalling gas. The parameter $T_{i,\mathrm{inf}}$ will be allowed to vary in order to find the best agreement with the present time observables (abundances, SFR and stellar mass). The SFR is a Schmidt–Kennicutt law:

$$\dot{\sigma}_{\mathrm{gas}} = \nu \sigma_{\mathrm{gas}}^{k} \quad (2)$$

with $k = 1$ as in previous papers (Ballero et al. 2007; Cescutti & Matteucci 2011; GMPC12). The quantity ν is the efficiency of star formation, namely the SFR per unit mass of gas, and for the bulge is assumed to be high relative to that normally assumed in the solar vicinity ($\nu = 1\,\mathrm{Gyr}^{-1}$, see for example Chiappini et al. 1997), thus simulating a starburst. The efficiency of star formation is in units of time^{-1} and represents the inverse of the time-scale in which all the gas is consumed. This approach was first suggested by Matteucci & Brocato (1990) and then proven to be required for reproducing the bulge properties in all the following papers dealing with the chemical evolution of the bulge. Here we assume several values for this parameter varying from ν from 20 to 200 Gyr^{-1}.

We explore different initial mass functions (IMFs), in particular:

(i) the one suggested by Ballero et al. (2007):

$$\phi_{\mathrm{B}}(M) = A_{\mathrm{B}} M^{-(1+x)} \quad (3)$$

with $x = 0.95$ for $M > 1\,\mathrm{M}_{\odot}$ and $x = 0.33$ for $M < 1\,\mathrm{M}_{\odot}$ in the mass range 0.1–100 $\mathrm{M}_{\odot}$ and $A_{\mathrm{B}} = 0.078$.

(ii) The normal Salpeter (1955) IMF ($x = 1.35$ in equation 3) in the mass range 0.1–100 $\mathrm{M}_{\odot}$, with $A_S = 0.17$.

(iii) The three-slope Kroupa, Tout & Gilmore (1993) IMF:

$$\phi_{\rm K}(M) = \begin{cases} A_{\rm K}\, M^{-0.3} & \text{if } M < 0.5\,{\rm M}_\odot \\ B_{\rm K}\, M^{-1.2} & \text{if } 0.5 < M/{\rm M}_\odot < 1 \\ C_{\rm K}\, M^{-1.7} & \text{if } M > 1\,{\rm M}_\odot \end{cases} \quad (4)$$

with $A_{\rm K} \approx 0.19, B_{\rm K} = C_{\rm K} \approx 0.31$.

(iv) The Chabrier (2003) IMF:

$$\phi_{\rm C}(M) = \begin{cases} A_{\rm C}\, {\rm e}^{-({\rm log}M - {\rm log}M_{\rm c})^2/2\sigma^2} & \text{if } M < 1\,{\rm M}_\odot \\ B_{\rm C}\, M^{-1.3} & \text{if } M > 1\,{\rm M}_\odot \end{cases} \quad (5)$$

with $A_{\rm C} \approx 0.85, B_{\rm C} \approx 0.24, \sigma = 0.69$ and $M_{\rm c} = 0.079$.

We note that this IMF is very similar to that of Kroupa (2001).

2.1 Nucleosynthesis and stellar evolution prescriptions

The nucleosynthesis prescriptions adopted here are different from those in GMPC12 and are the same as in Romano et al. (2010): they take into account the most recent calculations and have been tested on the chemical evolution of the solar neighbourhood and found to be the best ones.

In particular, the prescriptions for different stellar mass ranges are as follows.

(i) The yields of Karakas (2010) for low- and intermediate-mass stars ($0.8 \leq M/{\rm M}_\odot \leq 8$, LIMS), who has recomputed Karakas & Lattanzio's (2007) models with updated nuclear reaction rates and enlarged the grid of masses and metallicities.

(ii) The yields for massive stars ($M > 8\,{\rm M}_\odot$) are taken from Kobayashi et al. (2006), which included metallicity-dependent mass-loss, plus the yields of the Geneva group for C, N, O (Meynet & Maeder 2002a; Hirschi, Meynet & Maeder 2005; Hirschi 2007; Ekström et al. 2008), limited to the pre-supernova stage, but computed with both mass-loss and rotation.

(iii) The yields from Type Ia SNe are assumed to originate from exploding white dwarfs in binary systems and are taken from Iwamoto et al. (1999). The SN Ia rate is computed as in the previous papers (Ballero et al. 2007; Cescutti & Matteucci 2011; GMPC12) by assuming the single-degenerate model, as described in Greggio & Renzini (1983) and Matteucci & Recchi (2001). This particular formulation, namely the single-degenerate scenario, gives results very similar to the double-degenerate scenario for the progenitors of SNe Ia, as shown by Matteucci et al. (2006, 2009).

3 OBSERVATIONS

3.1 Abundances

The nine M-type giants in the GC region discussed here were analysed in Ryde & Schultheis (2015) using high spectral resolution in the K band, centred at 2.1 μm. They were selected using the Nishiyama et al. (2009) data set and the 3D interstellar extinction maps of Schultheis et al. (2014) to ensure that these giants are situated in the GC region. The low-resolution K-band spectra were used to determine the effective temperatures ($T_{\rm eff}$) with a precision of approximately 100 K. The surface gravities ($\log g$), were determined by adopting a mean distance of 8 kpc and using dereddened H and Ks magnitudes from the VVV survey of Minniti et al. (2010), resulting in a precision of less than 0.3 dex.

The high-resolution spectra, centred at 2.1 μm, were used to determine the metallicity ([Fe/H]) from several Fe lines and the Ca, Si and Mg abundances from several atomic lines. To derive the abundances, spectral synthesis was used with the software Spectroscopy Made Easy (Valenti & Piskunov 1996, 2012), based on MARCS spherical-symmetric, local thermodynamic equilibrium (LTE) model atmospheres (Gustafsson et al. 2008). The abundance from an observed spectral line was found by minimizing the χ^2, calculated from the comparison between synthetic spectra and the observations. The best fit was found, with the abundance as a free parameter, by minimizing the χ^2. The microturbulence of $\xi_{\rm micro} = 2.0 \pm 0.5\,{\rm km\,s^{-1}}$ was used in the analysis.

The uncertainties, due to the uncertainties in the fundamental parameters ($T_{\rm eff}$, $\log g$, [Fe/H] and $\xi_{\rm micro}$), in the derived metallicities and abundance ratios are of the order of 0.10–0.15 dex. There might also be unknown systematic uncertainties, such as non-LTE effects, but since the standard red giant star, Arcturus, is among the analysed stars and gives reasonable results, these uncertainties cannot be large. Unknown blends might also exist, especially for metal-rich stars, and will tend to overestimate the metallicities. However, the line blending is less severe in the K band compared to the optical region. Furthermore, since several Fe lines were used, this effect would rather lead to an increased dispersion in the abundances from the different lines. The molecules in the wavelength regions are predominantly due to CN, and are properly synthesized.

The metallicity distribution of Ryde & Schultheis (2015) agrees well with that of Cunha et al. (2007). These authors also measured Ca abundances, which also agree well with those measured by Ryde & Schultheis (2015).

3.2 The Central Molecular Zone

The understanding of the physical processes occurring in the nuclear disc of our Galaxy is crucial for the insight into the formation and evolution of our own Milky Way. The Central Molecular Zone (CMZ) is the innermost ∼200 arcmin region of the Milky Way. It covers about $-0.^\circ7 < l < 1.^\circ8$ in longitude and $-0.^\circ3 < b < 0.^\circ2$ in latitude which is within about 300 pc of the GC. It is a giant molecular cloud complex with an asymmetric distribution of molecular clouds (see e.g. Morris & Serabyn 1996; Martin, Walsh & Xiao 2004; Oka et al. 2005). Genzel et al. (2006) pointed out that most of the stars in the GC seem to have formed 9 ± 2 Gyr ago, probably at the same time as the Galactic bulge. Then the SFR dropped to a minimum a few Gyr ago and increased again in the past few million years. Recent *Herschel* observations (Molinari et al. 2011) show that the CMZ is a 100 pc elliptical and twisted ring of cold dust, with $3 \times 10^7\,{\rm M}_\odot$ of gas. This prodigious reservoir of molecular gas is an active region of star formation, with evidence of starburst activity in the last 10^5 yr (Yusef-Zadeh et al. 2009). The gas pressure and temperature are higher in the CMZ than in the average disc, conditions that favour a larger Jeans mass for star formation and an IMF biased towards more massive stars. Furthermore, the presence of strong magnetic fields, tidal shear and turbulence demonstrate that the conditions for star formation in the CMZ are significantly different from those in the Galactic disc (see Serabyn & Morris 1996; Fatuzzo & Melia 2009). From the observational point of view, the present SFR can be determined by counting massive young stellar objects (Immer et al. 2012).

In order to estimate bolometric luminosities from their flux densities at 15 μm, one has to correct for interstellar dust extinction (Schultheis et al. 1999). The total luminosity of the young stellar objects has then been converted to a total mass assuming a Salpeter IMF for masses in the range of 6–58 $\rm M_\odot$, while the low-mass objects ($M < 6.3\ {\rm M}_\odot$) have been converted using the Kroupa (2001) IMF.

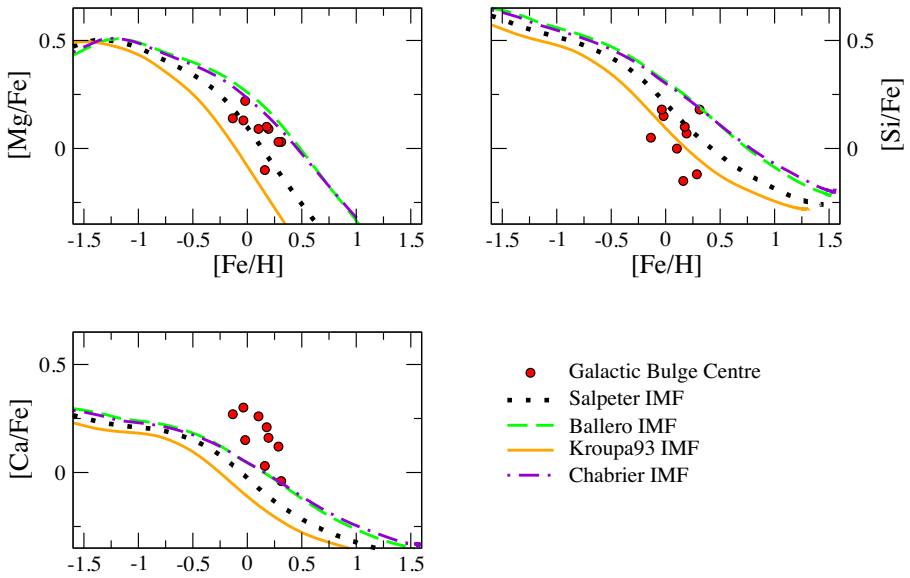

Figure 1. Predicted [Mg/Fe], [Si/Fe], [Ca/Fe] versus [Fe/H] for models with different IMFs, as indicated in the figure. The only parameter which varies from model to model is the IMF since each model has $\nu = 25$ Gyr^{-1} and $T_{i,\,\mathrm{inf}} = 0.7$ Gyr. The red filled circles are the abundances of GC stars from Ryde & Schultheis (2015).

In order to calculate the SFR, Immer et al. (2012) assumed a typical lifetime of 1 Myr for the young stellar objects which leads to an average SFR of 0.08 $M_\odot$ yr^{-1}. However, one has to take into account that the derived SFR are based on simple assumptions which could lead to significant errors. Previous studies (Yusef-Zadeh et al. 2009; Crocker 2011) published a range of values of 0.08−0.15 $M_\odot$ yr^{-1}. This is consistent with other studies using different tracers of gas and star formation activity leading to a present SFR of 0.04−0.15 $M_\odot$ yr^{-1} (Morris & Serabyn 1996; Yusef-Zadeh et al. 2009; Molinari et al. 2011 Immer et al. 2012) with a total gas mass of the order of $3-7 \times 10^7$ $M_\odot$. Given the total amount of gas in the CMZ, the SFR is by a factor of > 10 lower than expected. This suppression of star formation could be due to the high turbulent pressure (see e.g. Kruijssen et al. 2014). Pfhul et al. (2011) presented spatially resolved imaging and integral field spectroscopy for 450 cool giants within 1 pc from SgrA*. They derived the SFR of the nuclear cluster in the GC from the H–R diagram of the red giant population. They found that the SFR dropped from an initial maximum roughly 10 Gyr ago to a minimum at 1–2 Gyr ago and that increased again in the last few hundred million years. Their results imply that ∼80 per cent of the total stellar mass in the GC formed more than 5 Gyr ago.

4 RESULTS

4.1 Abundances

Two of the most important observational constraints to understand the most probable scenario for the bulge formation are the stellar MDF of stars and the [α/Fe] ratios. Originally, Matteucci & Brocato (1990) suggested that in order to fit the MDF of the bulge one should assume that it formed very quickly. The consequence of the fast formation is a particular [α/Fe] trend with supersolar values being present for a large interval of [Fe/H]. In other words, while in the solar vicinity the 'knee' of the [α/Fe] ratios occurs roughly at [Fe/H] ~ -1.0, in the bulge the knee appears at [Fe/H] ~ 0. This is due to the fact that in a regime of intense star formation, core-collapse SNe from massive stars enrich the ISM very fast in Fe (although they are not the main producers of this element), so when SNe Ia which produce the bulk of Fe occur, the abundance of Fe in the ISM is already almost solar (see Matteucci 2001, 2012).

We compare here the GC data with the chemical evolution model (hereafter the reference model) for a classical bulge of GMPC12. We computed several numerical models by varying the most important parameters: the IMF, the efficiency of star formation and the time-scale of the infalling gas. The reference model parameters are $\nu = 25$ Gyr^{-1}, $T_{i,\,\mathrm{inf}} = 0.1$ Gyr and the Salpeter IMF in agreement with the GMPC12G MP population. The data trend of Fig. 1 shows the effect of an intense burst of star formation coupled with the delay in the Fe production from SNe Ia: since star formation is very intense, the bulge very soon reaches a solar metallicity because of the core-collapse SN explosions, which produce part of the Fe. After a time delay necessary to the evolution of the binary system progenitors of SNe Ia, these SNe, which produce the bulk of Fe, start to explode changing the [α/Fe] slope at a larger [Fe/H] than in the solar vicinity. The models in Fig. 1 show also the effect of varying the IMF: the Ballero IMF and the Chabrier IMF give very similar results since they are favouring massive stars compared to the Kroupa et al. (1993) and Salpeter (1955) IMFs. In particular, the Kroupa et al. (1993) IMF which has been derived for the solar vicinity does not reproduce either the [Mg/Fe] or the [Ca/Fe] ratios, although it could reproduce the [Si/Fe] abundances. On the other hand, the Salpeter (1955) IMF can reproduce the [Mg/Fe] and [Si/Fe] ratios. We note that none of the adopted IMFs can reproduce the high values of the [Ca/Fe] ratios. This could be due to the uncertainties still existing in the stellar yields of specific elements, but also to observational errors. The abundance data are, in fact, more sensitive to the yield uncertainties rather than to the IMF, whereas the stellar MDF is highly sensitive to the IMF.

In Fig. 2, we can see the effects of a different star formation efficiency on the [Mg/Fe], [Si/Fe], [Ca/Fe] versus [Fe/H] trends: the green solid line is the reference model while the black dashed line is a model with an intense initial starburst with efficiency $\nu = 200$ Gyr^{-1}. This very high efficiency is probably unrealistic

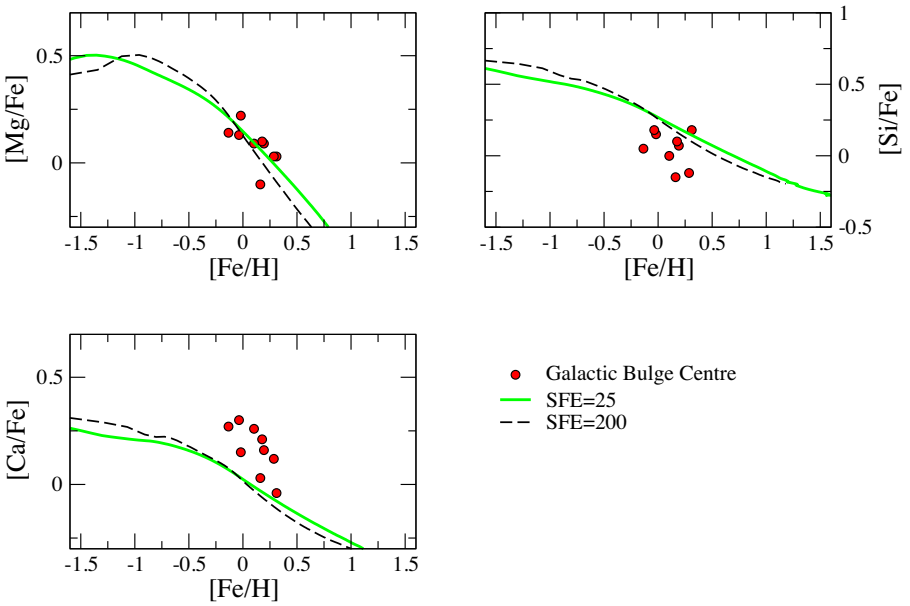

Figure 2. Predicted [Mg/Fe], [Si/Fe], [Ca/Fe] versus [Fe/H] by our fiducial model ($T_{i,\,\mathrm{inf}} = 0.1$ Gyr, Salpeter IMF) but with different star formation efficiency: $\nu = 25\,\mathrm{Gyr}^{-1}$ (green solid line) and $\nu = 200\,\mathrm{Gyr}^{-1}$ (black dashed line). The red filled circles are the abundances of GC stars measurements from Ryde & Schultheis (2015), as in Fig. 1.

since it predicts that the gas is consumed in 5 Myr. In any case, the differences among different models with $\nu = 25$ and 200 Gyr^{-1} are negligible. On the other hand, a $\nu = 1\,\mathrm{Gyr}^{-1}$ as in the solar vicinity (see Chiappini et al. 1997) would produce different results, in particular, all the curves would be translated at lower values of [α/Fe] ratios.

In Fig. 3, we show the effect of varying the infall time-scale. The differences among different models are small and from the figure we can conclude that a time-scale between 0.1 and 1.25 Gyr can be acceptable, whereas a time-scale of 0.01 Gyr seems too short.

In Fig. 4, we show the predicted stellar MDF for the fiducial model and the two different values of ν. Here, we can see that the effect of increasing ν results in a narrowing of the predicted MDF. It is worth noting that the number of observed stars in the GC is very small and therefore we do not aim at reproducing exactly the observed MDF but only at reproducing the position of the peak. The infall time-scales also affect the MDF and in Fig. 5 we show the predicted MDF for the Chabrier (2003) IMF and different infall time-scales; we note that for this IMF the infall time-scale of 0.1 Gyr produces results more in agreement with observations, while longer time-scales tend

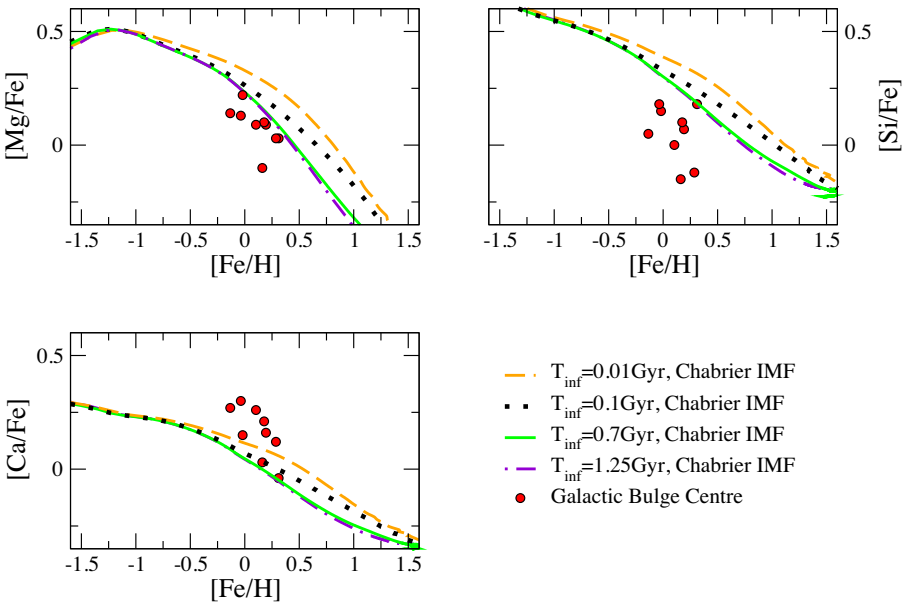

Figure 3. Predicted [Mg/Fe], [Si/Fe], [Ca/Fe] versus [Fe/H]. The only parameter which varies from model to model is the infall time-scale in the range $T_{i,\,\mathrm{inf}}$: 0.01–1.25 Gyr; we use the Chabrier IMF and the SFE of the fiducial model: $\nu = 25\,\mathrm{Gyr}^{-1}$. The red filled circles are the abundances of GC stars from Ryde & Schultheis (2015), as in Fig. 1.

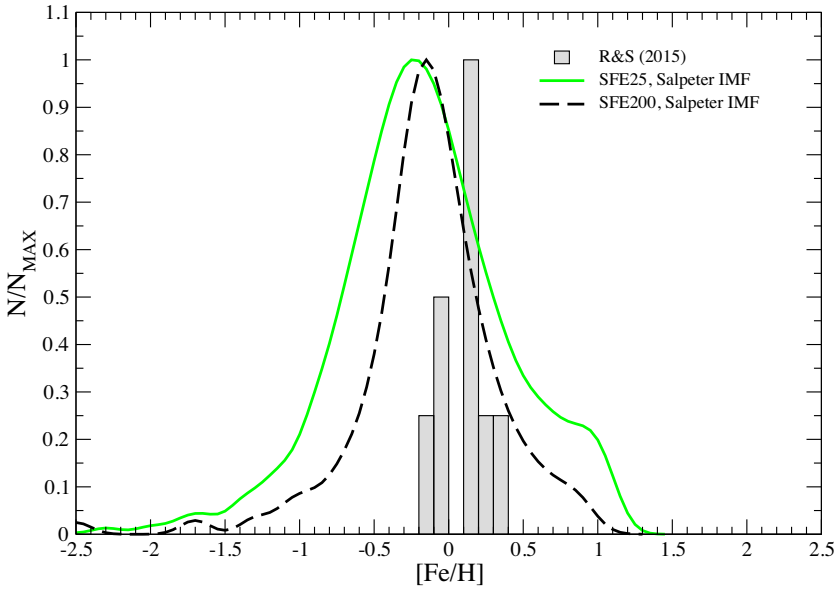

Figure 4. Predicted MDF for the fiducial model (green solid line) and a model with SFE $= \nu = 200$ Gyr^{-1} (black dashed line) as a function of [Fe/H]. The data are from Ryde & Schultheis (2015). The predicted MDFs have been convolved with a Gaussian with an error of 0.1 dex.

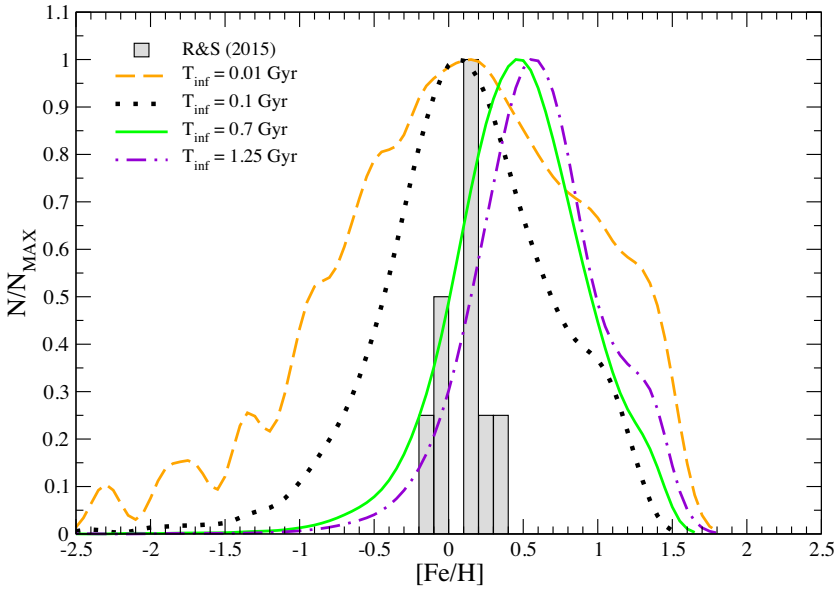

Figure 5. Predicted MDF for different models with star formation efficiency SFE $= \nu = 25$ Gyr^{-1} and the Chabrier IMF but with different infall time-scales. The lines have the same colour code as in Fig. 3. The data are from Ryde & Schultheis (2015). The predicted MDFs have been convolved with a Gaussian with an error of 0.1 dex.

to predict a peak at too high metallicities. Finally, in Fig. 6 we show the effect of varying the IMF on the predicted MDF, when the infall time-scale is fixed at 0.7 Gyr. In this case, we note that the Salpeter IMF produces the best agreement and predicts the peak of the MDF at the right position. However, given the small number of observed stars, we are not able to disentangle the degeneracy between IMF and infall time-scale. What seems more clear is that an IMF like Kroupa et al. (1993), good for the solar vicinity, predicts the worst agreement with data when both the abundance ratios and the MDF in the GC are taken into account. Previous models for the entire bulge (Matteucci & Brocato 1990; Ballero et al. 2007; Cescutti & Matteucci 2011; Kobayashi, Karakas & Umeda 2011) have supported an IMF which contains more massive stars than the one for the solar vicinity.

In summary, the comparison between data and model results suggests that the abundances in the GC are quite compatible with a fast formation of this region similarly to what happened to the entire bulge. The fact that the [α/Fe] ratios are low at high [Fe/H] is not necessarily a sign of prolonged star formation. Such a sign instead would be revealed by low [α/Fe] ratios at low [Fe/H], as happens in dwarf irregular galaxies and dwarf spheroidals where the SFR was quite mild. A regime of low star formation, in fact, produces a situation where the gas is still poor in Fe when Type Ia SNe start producing the bulk of this element. At this point,

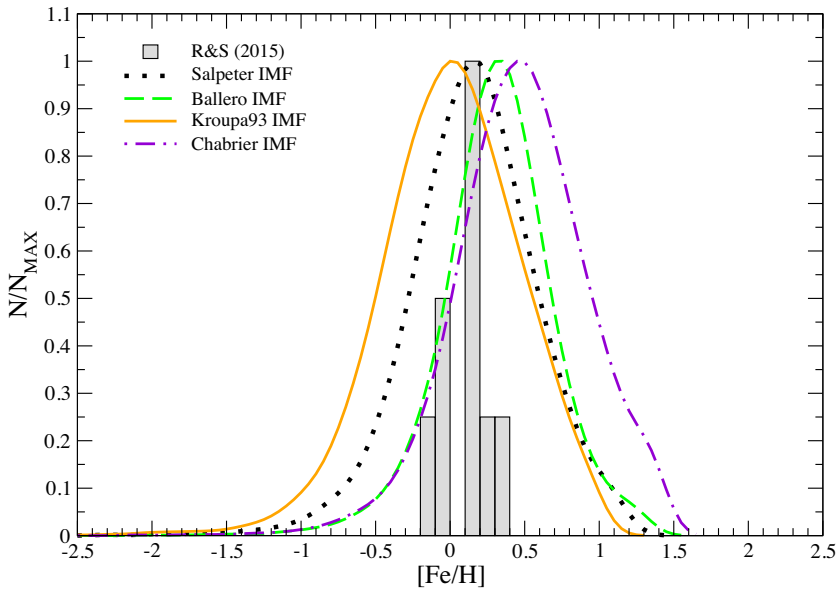

Figure 6. Predicted MDF for different models with star formation efficiency $\nu = 25\,\mathrm{Gyr}^{-1}$, infall time-scale $T_{i,\,\mathrm{inf}} = 0.7$ Gyr but with different IMFs; the lines have the same colour code of Fig. 1. The data are from Ryde & Schultheis (2015). The predicted MDFs have been convolved with a Gaussian with an error of 0.1 dex.

the [α/Fe] ratios start to decrease but the [Fe/H] is still low. The fact that the star formation was quite strong in the early phases of formation of the central region is also evident in the MDF which is peaked at high metallicity. However, we should keep in mind that the number of stars observed in the GC is not yet statistically significant and therefore firm conclusions cannot be drawn. We recall that in this section we have ignored the fact that recent star formation has been observed in the GC region, so in the next section we will explore the case in which a second burst has recently occurred and whether this recent SFR can affect our predictions.

4.2 Star formation in the GC

In our standard model for the GC, the bulk of the stars formed 10 Gyr ago and then the SFR decreased steadily until the present time to a value slightly lower than $10^{-4}\,\mathrm{M}_\odot\,\mathrm{yr}^{-1}$. Therefore, to reproduce the observations indicating active star formation at the present time, we have simulated a star formation history made up of a first strong burst, where most of stars formed (our fiducial model), plus a more recent starburst started 500 Myr ago. We have tested different cases and verified the effects of this second starburst on the [α/Fe] ratios and the MDF.

In order to simulate the second burst, we simply assumed a second gas infall episode which increased suddenly the available mass of gas:

$$\dot{\sigma}_{\mathrm{gas},i}(t) = A(r)X_{i,\mathrm{inf}}\mathrm{e}^{-t/T_{i,\mathrm{inf}}} + B(r)X_{i,\mathrm{inf}}\mathrm{e}^{-(t-t_{\mathrm{in}})/T_{\mathrm{inf}_2}}, \quad (6)$$

where t_{in} represents the cosmic time at which the second burst starts and T_{inf_2} is the infall time-scale of the second burst (see Table 1). The origin of this gas can be either extragalactic or coming from the inner regions of the Galactic disc thanks to the bar in the bulge.

We tested several cases but we show only the most realistic ones. In particular, we assumed: (i) a burst triggered by a strong infall of gas, comparable to the initial infall rate, (ii) a burst fuelled by a more modest infall of gas relative to the previous one and (iii) a starburst due only to a sudden increase of the star formation efficiency from 25 to 200 Gyr^{-1} without an extra-infall of gas. This case could simulate the effect of a nuclear bar, which simply compresses the existing gas. In the infall cases, we tested both primordial and metal enriched infall. We found that the best model is model (ii) with a modest infall of new gas, which reproduces the estimated total mass of stars formed in the last 500 Myr ($\sim 10^7\,\mathrm{M}_\odot$) as well as the observed present time SFR (0.04–0.15 $\mathrm{M}_\odot\,\mathrm{yr}^{-1}$). In fact, in case (i) the strong infall produces changes in the [α/Fe] ratios which are not seen in the data: in particular, the infall dilutes the abundances of heavy elements thus producing an inversion in the [α/Fe] versus [Fe/H] plot showing very low [α/Fe] ratios at low [Fe/H], not observed in the data. On the other hand, simply increasing the star formation efficiency (model iii) does not allow us to reproduce the observed present time SFR nor the observed gas in the GC. This is because the gas was already low 500 Myr ago when the starburst was supposed to start. Therefore, we suggest that this burst in the GC must have been triggered by accretion of new gas. The characteristics of the models (i), (ii) and (iii) are reported in Table 1, where we show the time-scale for the main infall episode ($T_{i,\,\mathrm{inf}}$), the star formation efficiency for this episode (SFE_1), the time-scale for the infall giving rise to the second burst (T_{inf_2}) and the star formation efficiency in this second burst (SFE_2).

Table 1. Parameters used for the two infall models: $T_{i,\,\mathrm{inf}}$ and T_{inf_2} are the infall time-scale of the two SF episodes expressed in Gyr, SFE_1 and SFE_2 are the star formation efficiencies in unit of Gyr^{-1} and finally t_{in} is the time of the second infall onset. For model (iii) there is no second infall but just a sudden increase of the star formation efficiency passing from 25 to 50 Gyr^{-1} at 13.2 Gyr.

Model	$T_{i,\,\mathrm{inf}}$ (Gyr)	SFE_1 (Gyr^{-1})	T_{inf_2} (Gyr)	SFE_2 (Gyr^{-1})	t_{in} (Gyr)
(i)	0.1	20	1	0.3	13.2
(ii)	0.1	25	1	20	13.2
(iii)	0.1	25	–	50	–

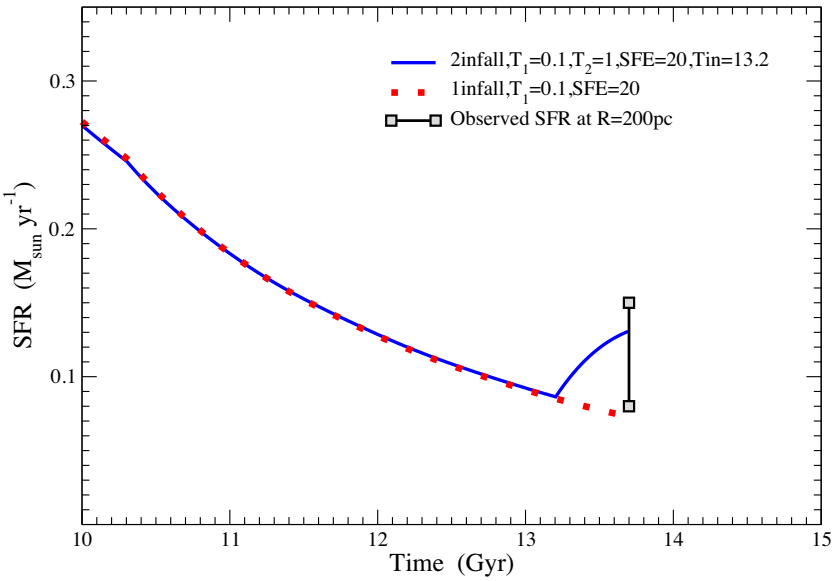

Figure 7. The star formation history of the GC in the last few billion years. The predicted SFR in $M_{\odot}\,yr^{-1}$ is given as a function of the galactic time in the case with a second starburst starting 500 Myr ago (model ii continuous line). The dashed red line indicates the model without any second burst of star formation. The adopted IMF in the models is that of Chabrier. The observed minimum and maximum SFR in the GC are marked (see text).

Finally, in column 6 the values of t_{in} (the time at which the second infall starts) is reported. The best model appears to be model (ii): it predicts a total mass of stars formed of $\sim 3.2 \times 10^7\,M_{\odot}$ and a present time SFR of $\sim 0.125\,M_{\odot}\,yr^{-1}$, in good agreement with the observed values. In Fig. 7, we show the predicted SFR history for model (ii) and we report also the observations.

In Fig. 8, we show the [α/Fe] ratios resulting from model (i) and (ii) which represent the case with a burst triggered by a strong gas infall and a modest gas infall, respectively. In the same figure also shown is an intermediate case showing that the inversion in the abundances, due to the dilution by infall, is independent of the onset time of the second strong burst. As one can see, a starburst triggered by a modest episode of primordial gas infall (at an average rate of $\sim 1.0\,M_{\odot}\,yr^{-1}$), occurring in the last hundred million years and reproducing the present time SFR, produces negligible effects on the predicted [α/Fe] ratios. On the other hand, as already mentioned, a second starburst triggered by a strong infall of gas (with an initial rate of $\sim 200\,M_{\odot}\,yr^{-1}$) would produce a noticeable but not observed effect in the data, even if the number of stars formed is the same. This case is clearly unrealistic since there is no physical justification for a strong late infall of primordial gas, but we show the resulting [α/Fe] ratios for the sake of comparison with case (ii). Moreover, it

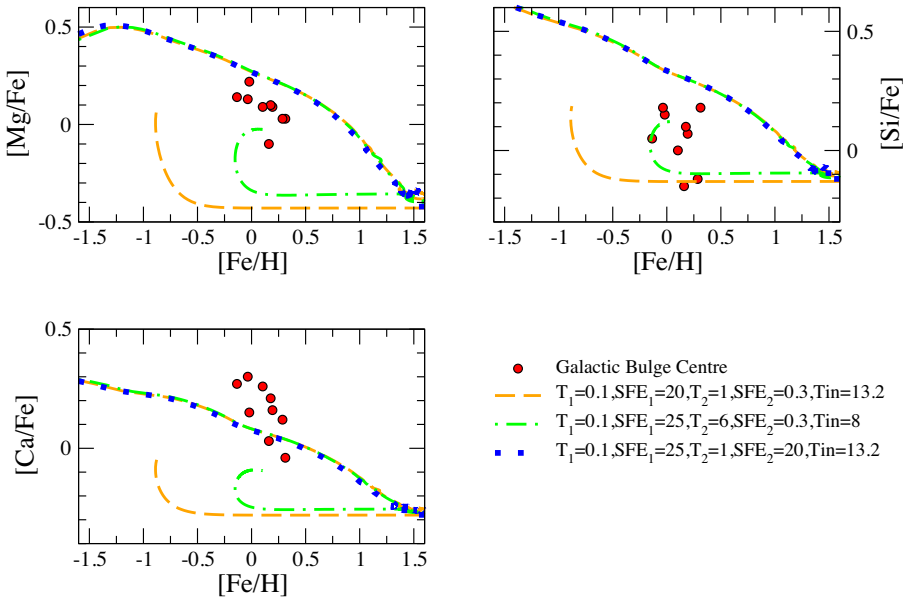

Figure 8. Predicted and observed [α/Fe] ratios for the following cases: the second burst of star formation triggered by a modest gas infall (model ii) indicated by the short dashed blue line, strong infall of gas comparable to the initial one indicated by the long-dashed yellow line. Finally, the dash–dotted green line indicates a model with the second burst triggered by a strong infall but starting at 8 instead of 13.2 Gyr. In the figure, are shown the parameters adopted in the three models in order to obtain acceptable values for the SFR at the present time.

is clear from Fig. 8 that none of the models with a late strong infall fits the data. We note that in all these cases we have chosen the model parameters to obtain acceptable values of the present time SFR as well as the total mass of stars formed. To do that we varied the star formation efficiencies and the infall time-scale. The reason for the inversion in the [α/Fe] ratios is therefore only due to the gas infall and to the way in which chemical elements are produced and on which time-scales. In particular, when a starburst is overimposed on a very low star formation regime, triggered by a huge episode of gas accretion, the abundances present at the moment in the ISM tend to be diluted by the infall, especially if the infalling gas is primordial, but at the same time they increase because of the new star formation. Therefore, according to the predominance of one or the other process, the abundances tend to increase or decrease. In our cases the abundances of Fe and the α-elements initially tend to decrease because of the infall, thus producing a reverse trend at constant [α/Fe], then as a result of the new production of α-elements by Type II SNe, the [α/Fe] ratios increase strongly. This is also due to the fact that Fe is not increasing immediately at the beginning of the second burst for the simple reason that Fe is mainly produced on long time-scales by Type Ia SNe. No stars seem to be observed with the [α/Fe] and [Fe/H] values predicted by the models with a late second starburst triggered by a huge gas infall. Only a model with a second very early starburst would not affect the [α/Fe] ratios, as expected. This fact suggests that a strong burst like the one we have hypothesized in model (i) cannot have occurred, otherwise it would have left a clear signature in the abundance pattern, and we have verified that this is true also for enriched infall. On the other hand, a minor burst triggered by either primordial or pre-enriched gas (enriched in metals) would produce negligible effects on the stellar abundances, as we have shown in Fig. 8. Concerning the MDF we tested model (ii) and no differences were produced by the second infall.

5 DISCUSSION AND CONCLUSIONS

In this paper, we have studied the chemical evolution of the central region of the Galactic bulge (200 pc radius) and compared our results with the recent data from Ryde & Schultheis (2015) concerning α-elements and Fe and the present time SFR (Morris & Serabyn 1996; Yusef-Zadeh et al. 2009; Molinari et al. 2011; Immer et al. 2012). We have tested different IMFs, efficiencies of star formation and infall time-scales. We also assumed a recent and ongoing burst of star formation where $\sim 3.2 \times 10^7$ M$_\odot$ of new stars formed.

Our main conclusions can be summarized as follows.

(i) A comparison between data and models suggests that the [α(Mg,Si,Ca)/Fe] ratios in the GC can be reproduced by a model assuming a strong star formation at the beginning such as that assumed for the whole bulge by previous models (Matteucci & Brocato 1990; Ballero et al. 2007; Cescutti & Matteucci 2011; GMPC12). Under this assumption, most of the stars in the GC have formed at the beginning (more than 10 Gyr ago) and the SFR has decreased steadily until the present time.

(ii) For [Mg/Fe] and [Si/Fe], we can conclude that a classical Salpeter IMF can reproduce the data, whereas for Ca the data always lie above the predictions and this is true also for the other assumed IMFs. We conclude that for Ca there could be a problem with stellar yields. In fact, stellar yields of some elements are still uncertain: here, we have adopted the set of stellar yields, for stars of all masses, considered the best to reproduce the abundance patterns in the solar vicinity (Romano et al. 2010, where also a discussion on the uncertainties on stellar yields can be found).

(iii) We have varied the efficiency of star formation from 20 to 200 Gyr^{-1} and found practically no difference in the results concerning the [α/Fe] versus [Fe/H] relations, whereas the MDF allows us to exclude the efficiency of 200 Gyr^{-1}. Therefore, we conclude that the efficiency of star formation in the GC is similar to that inferred for the whole bulge (GMPC12), namely 20–25 Gyr^{-1}.

(iv) We have tested different IMFs: Salpeter, Chabrier, Ballero and Kroupa93 and found that Salpeter, Ballero and Chabrier IMFs are probably the best to describe the GC, in agreement with previous results for the whole bulge suggesting an IMF with more massive stars than in the solar vicinity (Matteucci & Brocato 1990; Ballero et al. 2007; Cescutti & Matteucci 2011; GMPC12); in fact, they produce the best fits of the [α/Fe] versus [Fe/H] relations as well as the MDF, at the same time. However, the Salpeter IMF requires an infall time-scale longer (0.7 Gyr) than the other two IMFs (0.1 Gyr) to fit the data. Given the uncertainties still existing in the data we are not able at the moment to solve this degeneracy and therefore to draw firm conclusions on this point, but we can say that the infall time-scale for the formation of the bulk of GC stars was short.

(v) We tested also the effect of changing the infall time-scale and varied this time-scale from 0.01 Gyr (practically a closed-box model) to 1.25 Gyr. Again, with the exception of Ca, for which all the model predictions lie below the data, the Mg and Si data are compatible with time-scales in the range 0.1–1.25 Gyr, whereas the MDF is compatible with a range 0.1–07 Gyr.

(vi) Finally, we tested the effects of a second very recent burst occurring in the last five hundred million years and having an SFR and a total amount of formed stars comparable to those observed. We have found that such a burst, if triggered by a new modest infall episode of gas of primordial composition, would not produce any noticeable effect in the [α/Fe] relations and the MDF. On the other hand, we tested also a case of a starburst triggered by a huge gas infall, still producing the same present time SFR and total mass of new stars, and found that in this case the [α/Fe] are strongly affected by the infall. In particular, we predict very low values of [α/Fe] ratios at low [Fe/H], which are not observed.

(vii) Therefore, we conclude that the stars in the GC formed very quickly with a star formation efficiency of $\sim$25 Gyr^{-1}, and that the IMF should contain a larger number of massive stars than the typical IMF for the solar vicinity, such as the Kroupa et al. (1993). In particular, the recent IMF of Chabrier (2003) seems to be preferred. The present time observed SFR in the GC can be explained by a second burst of star formation with the same efficiency as the previous one and the same IMF, triggered by a modest infall episode. This second burst would not produce evident effects on the abundance patterns nor on the MDF, and is compatible with gas accretion induced by the main bar in the bulge.

ACKNOWLEDGEMENTS

We acknowledge financial support from PRIN MIUR 2010-2011, project 'The Chemical and dynamical Evolution of the Milky Way and Local Group Galaxies', prot. 2010LY5N2T. NR acknowledges support from the Swedish Research Council, VR (project number 621-2014-5640), Funds from Kungl. Fysiografiska Sällskapet i Lund. (Stiftelsen Walter Gyllenbergs fond and Märta och Erik Holmbergs donation). NR acknowledges the supports from Knut och Alice Wallenbergs stiftelse. We thank I. J. Danziger for reading the manuscript. Finally, we thank an anonymous referee for his/her important suggestions which improved the paper.

REFERENCES

Alard C., 2001, A&A, 379, L44
Babusiaux C. et al., 2010, A&A, 519, A77
Ballero S. K., Matteucci F., Origlia L., Rich R. M., 2007, A&A, 467, 123
Bensby T. et al., 2011, A&A, 533, A134
Bensby T. et al., 2013, A&A, 549, 147
Cescutti G., Matteucci F., 2011, A&A, 525, 126
Chabrier G., 2003, PASP, 115, 763
Chiappini C., Matteucci F., Gratton R., 1997, ApJ, 477, 765
Crocker R. M., 2011, Proc. 25th Texas Symp. Relativistic Astrophysics, preprint (arXiv:1103.4523)
Cunha K., Sellgren K., Smith V. V., Ramirez S. V., Blum R. D., Terndrup D. M., 2007, ApJ, 669, 1011
Ekström S., Meynet G., Chiappini C., Hirschi R., Maeder A., 2008, A&A, 489, 685
Erwin P., 2004, A&A, 415, 941
Fatuzzo M., Melia F., 2009, PASP, 121, 585
Genzel R. et al., 2006, Nature, 442, 786
Gerhard O., Martinez-Valpuesta I., 2012, ApJ, 744, 8
Gonzalez O. A. et al., 2011, A&A, 530, 54
Greggio L., Renzini A., 1983, A&A, 118, 217
Grieco V., Matteucci F., Pipino A., Cescutti G., 2012, A&A, 548, 60 (GMPC12)
Gustafsson B., Edvardsson B., Eriksson K., Jørgensen U. G., Nordlund Å, Plez B., 2008, A&A, 486, 951
Hill V. et al., 2011, A&A, 534, 80
Hirschi R., 2007, A&A, 461, 571
Hirschi R., Meynet G., Maeder A., 2005, A&A, 433, 1013
Immer K., Schuller F., Omont A., Menten K. M., 2012, A&A, 537, 121
Iwamoto K., Brachwitz F., Nomoto K., Kishimoto N., Umeda H., Hix W. R., Thielemann F.-K., 1999, ApJS, 125, 439
Karakas A. I., 2010, MNRAS, 403, 1413
Karakas A., Lattanzio J. C., 2007, PASA, 24, 103
Kobayashi C., Umeda H., Nomoto K., Tominaga N., Ohkubo T., 2006, ApJ, 653, 1145
Kobayashi C., Karakas A. I., Umeda H., 2011, MNRAS, 414, 3231
Kroupa P., 2001, MNRAS, 322, 231
Kroupa P., Tout C. A., Gilmore G., 1993, MNRAS, 262, 545
Kruijssen J. M. D., Longmore S. N., Elmegreen B. G., Murray N., Bally J., Testi L., Kennicutt R. C., 2014, MNRAS, 440, 3370
Laine S., Shlosman I., Knapen J. H., Peletier R. F., 2002, ApJ, 567, 97
Martin C. L., Walsh W. M., Xiao K., 2004, ApJS, 150, 239
Matteucci F., 2001, Astrophysics and Space Science Library, Vol. 253, The Chemical Evolution of the Galaxy. Kluwer, Dordrecht
Matteucci F., 2012, Astronomy and Astrophysics Library: Chemical Evolution of Galaxies. Springer-Verlag, Berlin
Matteucci F., Brocato E., 1990, ApJ, 365, 539
Matteucci F., Recchi S., 2001, ApJ, 558, 351
Matteucci F., Panagia N., Pipino A., Mannucci F., Recchi S., Della Valle M., 2006, MNRAS, 372, 265
Matteucci F., Spitoni E., Recchi S., Valiante R., 2009, A&A, 501, 531
Meynet G., Maeder A., 2002a, A&A, 390, 561
Minniti D. et al., 2010, New Astron., 15, 433
Molinari S. et al., 2011, ApJ, 735, L33
Morris M., Serabyn E., 1996, ARA&A, 34, 645
Nishiyama S. et al., 2005, ApJ, 621, L105
Nishiyama S., Tamura M., Hatano H., Kato D., Tanabé T., Sugitani K., Nagata T., 2009, ApJ, 696, 1407
Oka T., Geballe T. R., Goto M., Usuda T., McCall B. J., 2005, ApJ, 632, 882
Pfuhl O. et al., 2011, ApJ, 741, 108
Robin A. C., Marshall D. J., Schultheis M., Reylé C., 2012, A&A, 538, 106
Romano D., Karakas A. I., Tosi M., Matteucci F., 2010, A&A, 522, 32
Ryde N., Schultheis M., 2015, A&A, 573, AA14
Salpeter E. E., 1955, ApJ, 121, 161
Schultheis M. et al., 1999, A&A, 349, L69
Schultheis M. et al., 2014, A&A, 566, 120
Serabyn E., Morris M., 1996, Nature, 382, 602
Sersic J. L., 1968, Atlas de galaxias australes. Observatorio Astronomico, Cordoba, Argentina
Uttenthaler S., Schultheis M., Nataf D. M., Robin A. C. Lebzelter T., Chen B., 2012, A&A, 546, 57
Valenti J. A., Piskunov N., 1996, A&AS, 118, 595
Valenti J. A., Piskunov N., 2012, Astrophysics Source Code Library, record ascl:1202.013
Yusef-Zadeh F. et al., 2009, ApJ, 702, 178

This paper has been typeset from a TEX/LATEX file prepared by the author.